NIH Public Access
Author Manuscript
Circulation. Author manuscript; available in PMC 2014 September 10.

Published in final edited form as:
Circulation. 2011 October 25; 124(17): 1838–1847. doi:10.1161/CIRCULATIONAHA.111.032680.

Cardiomyocyte-Specific Deletion of the Vitamin D Receptor Gene Results in Cardiac Hypertrophy

Songcang Chen, MD, **Christopher S. Law, BS**, **Christopher L. Grigsby, BS**, **Keith Olsen, BS**, **Ting-Ting Hong, MD, PhD**[*], **Yan Zhang, MD, PhD**[*], **Yerem Yeghiazarians, MD**[*], and **David G. Gardner, MD**[*]

Diabetes Center and *Department of Medicine, University of California at San Francisco, San Francisco, CA 94143-0540

Abstract

Background—A variety of studies carried out using either human subjects or laboratory animals suggest that vitamin D and its analogues possess important beneficial activity in the cardiovascular system. Using Cre-Lox technology we have selectively deleted the vitamin D receptor (VDR) gene in the cardiac myocyte in an effort to better understand the role of vitamin D in regulating myocyte structure and function.

Methods and Results—Targeted deletion of exon 4 coding sequence in the VDR gene resulted in an increase in myocyte size and left ventricular weight/body weight versus controls both at baseline and following a 7-day infusion of isoproterenol. There was no increase in interstitial fibrosis. These knockout mice demonstrated a reduction in end diastolic and end systolic volume by echocardiography, activation of the fetal gene program (i.e. increased atrial natriuretic peptide and alpha skeletal actin gene expression) and increased expression of MCIP 1, a direct downstream target of calcineurin/NFAT signaling. Treatment of neonatal cardiomyocytes with 1,25- dihydroxyvitamin D partially reduced isoproterenol-induced MCIP 1 mRNA and protein levels and MCIP 1 gene promoter activity.

Conclusions—Collectively, these studies demonstrate that the vitamin D-VDR signaling system possesses direct, anti-hypertrophic activity in the heart. This appears to involve, at least in part, suppression of the pro-hypertrophic calcineurin/NFAT/MCIP 1 pathway. These studies identify a potential mechanism to account for the reported beneficial effects of vitamin D in the cardiovascular system.

Keywords

Vitamin D Receptor; Gene deletion; Isoproterenol; Cardiac hypertrophy

Address correspondence to: Songcang Chen, M.D., Diabetes Center UCSF, 1119 HSW 513 Parnassus Ave, San Francisco, CA 94143-0540, Tel (415) 476-2729 FAX (415) 564-5813, schen@diabetes.ucsf.edu.

Publisher's Disclaimer: This is a PDF file of an unedited manuscript that has been accepted for publication. As a service to our customers we are providing this early version of the manuscript. The manuscript will undergo copyediting, typesetting, and review of the resulting proof before it is published in its final citable form. Please note that during the production process errors may be discovered which could affect the content, and all legal disclaimers that apply to the journal pertain.

Disclosures

We have no conflicts to disclose.

NIH-PA Author Manuscript
NIH-PA Author Manuscript
NIH-PA Author Manuscript

NIH-PA Author Manuscript

NIH-PA Author Manuscript

NIH-PA Author Manuscript

Vitamin D is ingested in the diet or generated *de novo* through scission of cholesterol precursors in the skin by ultraviolet light[1]. Once formed, vitamin D is activated through two sequential hydroxylation reactions. The first of these, a 25-hydroxylation, takes place largely in the liver to produce 25 hydroxyvitamin D. This molecule circulates bound to a plasma protein and is the form that is measured to assess the adequacy of vitamin D stores in the organism. The second hydroxylation, a 1 α hydroxylation, takes place in a variety of tissues, including the kidney, to generate 1,25 dihydroxyvitamin D [1,25 $(OH)_2$ D], the most polar and biologically active of the vitamin D metabolites. 1,25 $(OH)_2$ D functions as a ligand for the nuclear vitamin D receptor (VDR) which, when paired with its heterodimeric retinoid X receptor (RXR) partner, binds to sequence-specific recognition elements on DNA and stimulates or represses transcription of contiguous genes[2].

The prevalence of vitamin D deficiency and insufficiency (i.e. plasma levels of 25-hydroxyvitamin D <20 and <30 ng/ml, respectively) is estimated at greater than one billion people worldwide[1]. In developed countries it is seen more commonly in otherwise normal individuals with dark skin pigmentation, older individuals, obese individuals and individuals living at higher latitudes particularly during the winter months[1, 3]. Vitamin D insufficiency has been shown to cluster with a variety of cardiovascular and metabolic disorders of clinical importance including hypertension[4–6], insulin resistance[7], metabolic syndrome[8], diabetes mellitus[9, 10], peripheral vascular disease[11] and congestive heart failure[12, 13] raising the intriguing possibility of a mechanistic link between vitamin D insufficiency and cardiovascular disease.

A limited number of interventional studies have linked vitamin D repletion to reduction in blood pressure[14, 15] in humans, and the use of 1,25 $(OH)_2$ D and its bioactive analogues has led to reversion of cardiac hypertrophy in rats[16] and in patients with end stage renal failure on dialysis[17].

We have shown previously that the liganded VDR displays anti-hypertrophic activity in neonatal rat ventricular myocytes in culture[18]. Recent studies from Li and colleagues have shown that the VDR gene-deleted ($VDR^{-/-}$) mouse displays both hyper-reninemic hypertension[19] and ventricular hypertrophy[20]. The presence of hypertension and inferred increased ventricular afterload make it difficult to assign this anti-hypertrophic activity to VDR-signaled events within the myocyte itself. The presence of secondary hyperparathyroidism in these mice[21] and the postulated link between parathyroid hormone excess and cardiovascular dysfunction[22] add to the complexity of data interpretation in this model. In an effort to address this issue in a directed fashion, we have generated a mouse with selective deletion of the VDR gene in the myocytes of the heart and shown that these mice demonstrate increased cardiac hypertrophy both at baseline and following administration of isoproterenol (ISO), a hypertrophic stimulus.

Methods

Cardiomyocyte-specific VDR knockout mice

Generation and characterization of a floxed VDR targeting construct, transfection into embryonic stem cells and introduction of these cells into mice are described in the Methods

NIH-PA Author Manuscript

NIH-PA Author Manuscript

NIH-PA Author Manuscript

section of the Online-Only Data Supplement. The recombinant VDR allele bearing the loxP-bordered exon 4 was maintained in the C57/BL6J background. The neomycin resistance gene cassette was excised through a cross with the Flpe mouse[23]. Mice harboring the recombinant allele ($VDR^{loxP/loxP}$ or $VDR^{loxP/-}$) were bred with MLC-Cre[24] or Sox2-Cre mice[25] to create cardiomyocyte-specific or global VDR knockout mice, respectively. All experiments were carried out in mice at ~ 6 months of age. All animal-related experimental protocols were approved by the Institutional Animal Care and Use Committee at University of California San Francisco.

ISO infusion and blood pressure measurement

Mice were anesthetized with 1.5% isoflurane and subcutaneous Alzet osmotic minipumps containing PBS or ISO, the latter calibrated to release drug at the rate of 15 mg/kg/d for 7 days, were surgically implanted subcutaneously in the interscapular region of the mouse. Mouse blood pressure was measured using the tail-cuff method. Mice were trained on the Hatteras Instruments SC1000 Blood Pressure Analysis System, used according to manufacturer's instructions, for 4 days. Ten consecutive measurements on the last day were averaged to calculate systolic and diastolic blood pressure. Mean arterial blood pressure was calculated as 2/3 diastolic pressure plus 1/3 systolic blood pressure.

Ventricular myocyte isolation and cell sorting

Adult mouse ventricular myocytes were isolated using a previously described retrograde perfusion technique[26] with minor modification. The detailed procedure for isolation of the myocytes is described in the Methods section of the Online-Only Data Supplement. To purify myocytes further, cells were sorted at a flow rate of 250 cells/s on a MoFlo cytometer (Beckman Coulter, Brea, CA) using a 100-μm tip and a 488-nm Argon laser for excitation. Rod-shaped cardiac myocytes were sorted using the following sort parameters: autofluorescence (excitation at 488 nm; emission at 525 nm), cell size (high forward and sidescatter) and cell length >128 on 0–256 linear scale (time of flight based on both Pulse Width and Integrated Pick signals).

Echocardiography

Mice were anesthetized with 1.5% isoflurane and transthoracic echocardiography was performed using a Vevo 660 system (VisualSonics, Toronto, Canada) equipped with a 30-MHz transducer according to the methods of Zhang et al.[27]. Left ventricular ejection fraction (LVEF), end-systolic volume (ESV), end-diastolic volume (EDV), and wall thickness were assessed at different time points accordingly. Diastolic function parameters, including peak early (E) and late (A) mitral inflow velocities, were measured. Three cycles were measured for each assessment, and the average values were obtained. Analyses of the echocardiographic images were performed in a blinded manner.

Tissue harvesting, histology and morphormetrical analyses

Mice were weighed and sacrificed. The atria and right ventricular free walls were dissected away from the left ventricle. The left ventricles, including septum, were weighed, quick frozen and stored at −80 °C for later preparation of DNA and RNA. Selected mice were

NIH-PA Author Manuscript

NIH-PA Author Manuscript

NIH-PA Author Manuscript

deeply anesthetized, and the hearts were perfused with saline followed by Z-Fix (Anatech Ltd, Battle Creek, MI). Fixed left ventricles were embedded in paraffin, and cross sections were stained with hematoxylin and eosin (H&E) or Masson's trichrome to evaluate gross morphology and cardiac fibrosis. To quantify individual myocyte size, some sections were stained with fluorescein isothiocyanate-conjugated wheat germ agglutinin (FITC-WGA), as described by Xu et al.[28]. Myocyte area was assessed with ImageJ (NIH) with the investigator blinded to the genotype. The mean cardiomyocyte area was evaluated by measurement of 400 cells per heart (4–5 hearts per genotype).

Plasma measurements

Plasma was collected at the time of sacrifice and used to measure total calcium (IDEXX Laboratories, West Sacramento, CA). Plasma PTH was measured using a mouse intact PTH ELISA kit (Immutopics, San Clemente, CA) and plasma ANP concentration was measured with a commercial radioimmunoassay kit (Phoenix Pharmaceutical, Mountain View, CA) according to the manufacturer's instructions.

Plasmid construction

An 852-bp segment of the MCIP 1 promoter in the intron region upstream of exon4 from mouse genome (Gene: Rcan1 (ENSMUSG00000022951) containing multiple NFAT binding sites[29] was amplified and subcloned into the KpnI and XhoI restriction sites in pGL3 vector (Promega, Madison, WI). The structure was confirmed by DNA sequencing.

Gene array and differential expression analysis

DNase-digested total RNA was isolated from the cardiomyocytes of wild type and myocyte-specific VDR knockout mice. Sample quality and quantity was determined by assaying samples in Bioanalyzer RNA Nano Assays (a RIN score above 8.5 was recorded for all samples) and with a Nanodrop Spectrophotometer (Thermo Fisher Scientific, Wilmington, DE). All samples were amplified using NuGEN Applause Plus kits (NuGEN Technologies Inc., San Carlos, CA), converted to sense strand DNA and then fragmented and labeled according to manufacturer's instructions. Samples were hybridized to Affymetrix Mouse Gene 1.0 ST arrays (Affymetrix, Santa Clara, CA), stained and scanned according to the manufacturer's protocols. A total of 26,581 known gene expression profiles were detected. Microarrays were normalized to control for array-specific effects using the Affymetrix Power Tools software with the Robust Multi-Array (RMA) normalization. The average signal intensity in our microarrays was 7.5 after normalization. For statistical analyses, all probe sets where none of the groups had an average log 2 intensity greater than 3.0 were removed. This is a standard cutoff, under which the expression levels are indistinguishable from background. All log values were log 2. Linear models were fitted for each gene using the Limma package (Smyth 2008) in R/Bioconductor. Moderated t-statistics and the associated P-values were calculated.

Genotyping, Southern blot analysis

Neonatal cardiomyocyte preparation, luciferase assay, real-time (RT)-PCR and Western blot analysis are presented in the Methods section of the Online-Only Supplement Material.

NIH-PA Author Manuscript

NIH-PA Author Manuscript

NIH-PA Author Manuscript

Statistical analysis

Data are expressed as mean ± SD. Data were analyzed using two-way ANOVA. Statistical significance ($p<0.05$) was assessed using the Newman-Keuls test.

Results

Using a strategy outlined in Fig. 1A, we engineered loxP sites around the fourth exon of the murine VDR gene and placed it in a targeting construct containing a neomycin resistance casette. The fourth exon was selected for deletion based on the phenotype of the whole animal knockout generated by Li and coworkers[21]. The targeting construct was transfected into SV/129 embryonic stem cells (Fig. 1B and C) which, in turn, were introduced into the blastocysts of C57/BL6J mice. Chimeric offspring were identified and screened for the recombinant allele. This allele was tracked in subsequent generations (at least 6 generations bred into the C57/BL6 background) using conventional PCR analysis of tail genomic DNA. Additional details on the generation of the $VDR^{loxP/loxP}$ mice are provided in the Methods section of the Online-Only Data Supplement and Supplemental Fig. 1A–D.

In an effort to document accurate positioning and accessibility of the loxP sites, we mated a Sox2-Cre transgenic mouse – which allows for ubiquitous expression of Cre in mice harboring this transgene – with mice homozygous for the recombinant floxed VDR allele ($VDR^{loxP/loxP}$). Subsequent derivatives of this cross showed complete elimination of exon 4 at the VDR gene locus, effectively confirming their genotype as $VDR^{-/-}$ (Fig. 1D). As shown in the supplemental data, $VDR^{-/-}$ mice demonstrated no immunoreactive VDR in extracts from tail tissue (vs. robust signal in wild type mice) (Supplemental Fig. 2A). They also displayed alopecia and reduced body weight (Supplemental Fig. 2B) as previously reported for mice homozygous for the VDR gene deletion[21]. This confirms both correct positioning and accessibility of the loxP sites in the targeted VDR gene allele.

When $VDR^{loxP/loxP}$ mice were mated with mice bearing a Cre recombinase, as a single copy gene knock-in under control of the myosin light chain gene promoter (MLC-Cre)[24], the observed efficiency of exon 4 deletion was less than 50% (Fig 1D), likely reflecting the fact that the majority of nuclear DNA in these preparations is derived from non-myocyte cells (e.g. interstitial fibroblasts) which would not be predicted to express the MLC-Cre gene. MLC-Cre-dependent excision was more obvious when we introduced one null allele into the VDR gene locus ($M^{-/-}$) (Fig. 1D right lane). To be more precise about the level of exon 4 deletion in the MLC-Cre/$VDR^{loxP/loxP}$ mice, we isolated individual myoctes from these hearts as well as those from animals bearing the uncut recombinant floxed allele ($VDR^{loxP/loxP}$) and carried out the same PCR analysis. As shown in Fig. 1E, there was ~ 90% efficiency in the excision of exon 4 in myocytes of the MLC-Cre/$VDR^{loxP/loxP}$ mice.

To maximize the efficiency of the proposed myocyte-specific VDR gene excision, we mated the $VDR^{loxP/loxP}$ mouse with the heterozygous whole animal knockout ($VDR^{+/-}$) to generate the $VDR^{loxP/-}$ mouse (see Fig. 1D). This mouse, like the $VDR^{+/-}$ reported previously[21], does not appear to have phenotypic characteristics that differ from the wild type $VDR^{+/+}$ mouse (see below). Moving MLC-Cre into the $VDR^{loxP/-}$ background was predicted to effect near-complete deletion of the VDR gene in the cardiac myocytes. This was

NIH-PA Author Manuscript

NIH-PA Author Manuscript

NIH-PA Author Manuscript

documented by real time PCR analysis of RNA collected from these hearts as shown in Fig. 2A. While $VDR^{loxP/-}$, similar to $VDR^{+/-}$, displayed ~ 50% wild type cardiac VDR transcript levels, the cardiac selective VDR gene deletion displayed levels that were ~20% of wild type levels. The residual presumably reflects VDR expression in cardiac fibroblasts heterozygous for the wild type gene. Expression was greatly reduced (<5% of wild type cardiac VDR mRNA levels) in the partially purified myocytes and undetectable in myocytes that were further purified by cell sorting. To confirm VDR deletion in mouse cardiomyocytes, we further characterized the VDR mRNA products from the wild type and cardiac-specific VDR null myocytes. We reverse transcribed DNAse-digested mRNA isolated from wild type myocytes vs. myocytes collected from the cardiomyocyte specific VDR null hearts. VDR cDNA was amplified using a specific primer pair positioned in the exons 3 and 5. As shown in Supplemental Fig. 3A, a shorter VDR transcript was detected in cardiac-specific VDR-deleted myocytes while the wild type myocytes contained a transcript of the normal predicted size. Wild type and exon 4-deleted VDR cDNAs were purified from the gel and the cDNAs were sequenced. As expected, wild type VDR cDNA sequences were identical to the published sequence (http://uswest.ensembl.org/index.html; Transcript: VDR-001 [ENSMUST00000023119]) (Supplemental Fig. 3B). As shown in Suppl. Fig. 3C, deletion of exon 4 led to direct, out-of-frame fusion of exon 3 with exon 5 cDNA sequence. This fusion converts AGG (AG from exon 3 and G from exon 4) encoding arginine, to AGT (AG from exon 3 and T from exon 5) encoding serine. Furthermore, the fusion places a translation stop codon (TGA) in frame 4 amino acids further downstream (Supplemental Fig. 3C&D), implying that any protein translated through this fused carboxy terminal segment would be very significantly foreshortened (lacking the second zinc figer in the DNA binding domain and the whole hormone binding domain). Identical sequence was obtained using the cDNA transcribed from total mRNA isolated from the cardiomyocytes of global VDR knockout mice (data not shown). These results confirm wild type VDR gene expression in adult mouse cardiomyocytes and document the absence of VDR gene expression, assessed at the mRNA level, in cells harboring a cardiomyocyte-specific deletion of the VDR gene. Unlike the $VDR^{-/-}$ mice, the MLC-Cre/$VDR^{loxP/-}$ mice were not hypocalcemic on a standard chow diet (Fig. 2B), nor was hyperparathyroidism present (Fig. 2C), supporting the cardiac specificity of the deletion.

We next compared the morphology of hearts from MLC-Cre/$VDR^{loxP/-}$ mice with those of $VDR^{loxP/-}$ at baseline and following seven days of exposure to continuous ISO infusion, a maneuver which reliably generates myocardial hypertrophy in the mouse[30]. As shown in Fig. 3A and Table 1, at baseline hearts from the cardiac-specific knockout animals were larger than those from the $VDR^{loxP/-}$ controls. ISO infusion led to the expected increase in cardiac size in both the $VDR^{loxP/-}$ and the MLC-Cre/$VDR^{loxP/-}$ mice, but the increase in the latter was considerably more robust, approaching levels seen in the whole animal knockout ($VDR^{-/-}$) (see Supplemental Fig. 4A). The macroscopic changes in cardiac morphology were accompanied by hypertrophy of individual myocytes at the microscopic level. As shown in Fig. 3B and C, myocytes from the MLC-Cre/$VDR^{loxP/-}$ mice were significantly larger than those from the $VDR^{loxP/-}$ animals, in the presence or absence of ISO. Interestingly, this was not accompanied by an increase in interstitial fibrosis, as assessed by Masson's trichrome staining of myocardial tissue sections in Supplemental Fig. 5. Neither

NIH-PA Author Manuscript

NIH-PA Author Manuscript

NIH-PA Author Manuscript

MLC-Cre/VDR$^{loxP/-}$ mice nor VDR$^{loxP/-}$ mice displayed more than 1% collagen fraction in the sections examined. Heart size was unchanged in the MLC-Cre, VDR$^{loxP/loxP}$ or VDR$^{loxP/-}$ mice vs. the wild type littermates (see Supplemental Fig. 4A).

The morphological changes of cardiac hypertrophy were accompanied by increased expression of the fetal gene program which is typically associated with hypertrophy of neonatal and adult ventricular myocytes[31]. As shown in Fig. 4, expression of the atrial natriuretic peptide (ANP) (Panel A) or alpha skeletal actin (αSA) (Panel B), both representatives of the fetal gene program, was increased in the MLC-Cre/VDR$^{loxP/-}$ mice above those seen in the VDR$^{loxP/-}$. Expression of these genes at baseline in MLC-Cre/VDR$^{loxP/-}$ mice approached those levels achieved with ISO infusion in the VDR$^{loxP/-}$ mice. The combination of ISO in the MLC-Cre/VDR$^{loxP/-}$ mice led to at least an additive increase in fetal gene expression. Expression of ANP (Supplemental Fig. 4B) and αSA (Supplemental Fig. 4C) in MLC-Cre, VDR$^{loxP/loxP}$ or VDR$^{loxP/-}$ mice was not different from the wild type littermates.

The increment in heart size was confirmed by echocardiography in living mice (Fig. 5A and B). The MLC-Cre/VDR$^{loxP/-}$ mice displayed increased thickness of the interventricular septum and posterior left ventricular free wall relative to the VDR$^{loxP/-}$ controls, in the presence or absence of the ISO infusion, paralleling the gravimetic findings described above. There was a reduction in EDV and ESV in the MLC-Cre/VDR$^{loxP/-}$ mice (in the presence or absence of ISO) but no significant change in left ventricular systolic or diastolic function in the MLC-Cre/VDR$^{loxP/-}$ vs. VDR$^{loxP/-}$ mice (Supplemental Table 1).

As mentioned above, while the whole animal VDR gene knockouts (VDR$^{-/-}$) display cardiac hypertrophy[20], interpretation of this finding is complicated by the presence of hypertension in these animals. To provide assurance that blood pressure and, inferentially, ventricular afterload were not contributing to the development of left ventricular hypertrophy in the MLC-Cre/VDR$^{loxP/-}$ mice, we measured blood pressure in previously acclimated mice using the tail cuff technique[32]. As shown in Fig. 6A, the MLC-Cre/VDR$^{loxP/-}$ mice had lower diastolic and mean arterial blood pressure relative to the controls. While systolic blood pressure tended to be lower in these mice vs. controls, this difference did not reach statistical significance. The mechanism underlying the reduction in blood pressure remains unclear; however, increased ANP gene expression (Fig. 4A) and modestly increased ANP secretion (Fig. 6B) from the hearts of the MLC-Cre/VDR$^{loxP/-}$ mice might account for at least an element of the reduction in blood pressure. A similar mechanism has been suggested to account for the reduction in blood pressure noted following the myocyte-specific deletion of the type A natriuretic peptide receptor[33].

Global VDR-null mice[20] display an increase in renin gene expression in the heart. Renin expression was extremely low at baseline in the adult murine left ventricle. As shown in Supplemental Fig. 6., we did not detect increased renin expression in the left ventricles of cardiomyocyte-specific VDR knockout mice. These results suggest that local renin expression is unlikely to play an important role in the cardiac hypertrophy seen in the myocyte-specific, VDR deficient mice. Consistent with the findings of Li et al.[19], we did find increased renin expression in the kidneys of our VDR$^{-/-}$ mice (data not shown).

NIH-PA Author Manuscript

NIH-PA Author Manuscript

NIH-PA Author Manuscript

To explore the mechanism underlying myocyte hypertrophy in the cardiomyocyte specific VDR gene deleted mice, we performed gene array analysis using conventional hybridization array methodology. In comparing wild type with VDR-deleted cardiac myocytes (n=5 samples/group), we found that a limited number of genes (n=7) were upregulated more than 2-fold in the latter mice (Fig. 7A & Supplemental Fig. 7). One of these was the modulatory calcineurin inhibitory protein 1 (MCIP 1 or Rcan1), a gene product which functions as a downstream effector for calcineurin-dependent activity[34, 35]. Activation of calcineurin/ the Nuclear Factor of Activated T cells (NFAT) cascade has been linked to the development of pathological myocyte hypertrophy in several experimental models[34–41] and some forms of hypertrophy are abrogated in the MCIP $1^{-/-}$ mouse[34, 35]. Using real-time PCR analysis we confirmed that MCIP 1 expression was selectively increased in whole hearts from $VDR^{-/-}$ and myocyte specific VDR-deleted mice (Fig. 7 B&C). Using cultured neonatal rat ventricular myocytes, we showed that the hypertrophic agonist ISO increased MCIP 1 mRNA levels, MCIP 1 protein levels and MCIP 1 promoter activity, while pre-treatment with 1,25 $(OH)_2$ D resulted in partial inhibition of this induction (Fig. 8). These results imply that MCIP 1 is an important target of the liganded VDR in cardiomyocytes and suggest that antagonism of the calcineurin/NFAT/MCIP 1 signaling pathway plays a major role in defining the anti-hypertrophic activity of the liganded VDR.

Discussion

The studies reported here describe, for the first time, a direct role for the VDR in the antagonism of hypertrophic growth of the cardiac myocytes *in vivo*. This anti-hypertrophic activity may account for some fraction of the beneficial effects that the hormonal ligand for the VDR, 1,25 $(OH)_2$ D, is reported to have in the cardiovascular system[42].

Ventricular hypertrophy has been reported in the whole animal VDR gene knockout mouse ($VDR^{-/-}$)[20] but this is in the setting of 10–15 mm Hg elevations in systolic and diastolic blood pressure[19], systemic hyper-reninemia and the potential for dysregulated mineral homeostasis (e.g. lower calcium, and phosphate and elevated parathyroid hormone levels) in these mice compared with their wild type counterparts. Hyperparathyroidism has been linked to elevations in blood pressure[43] and cardiac hypertrophy[44] and in the studies of Park et al.[17], vitamin D-dependent reversion of cardiac hypertrophy correlated with reduction in parathyroid hormone levels. The hypertrophy seen in the cardiomyocyte-specific VDR knockout (Fig. 3) is somewhat less than that reported in the $VDR^{-/-}$ mouse[20]; however, given the differences in arterial blood pressure (i.e. estimated ~20 mm Hg difference in BP in the cardiac specific knockout vs. $VDR^{-/-}$), and the fact that the reduction in blood pressure-dependent afterload would be predicted to reduce the magnitude of the hypertrophic response, we are probably underestimating the true anti-hypertrophic effect of liganded VDR signaling in mice with the cardiomyocyte specific VDR deletion.

The anti-hypertrophic activity described here is likely to be one of a number of beneficial effects that vitamin D and its derivatives exert in the cardiovascular and renal systems. These agents have been shown to suppress proliferation of vascular smooth muscle cells in culture[45] and inhibit cholesterol sequestration in macrophages collected from patients with diabetes mellitus[46], both of which would be predicted to mitigate progression of vascular

NIH-PA Author Manuscript

NIH-PA Author Manuscript

NIH-PA Author Manuscript

lesions in diseases like atherosclerosis. The liganded VDR also reduces renin production[19, 20] which could lead to beneficial effects on blood pressure and vascular structural integrity.

The liganded VDR also suppresses proliferative and synthetic activity in the interstitial compartment (i.e. fibroblasts and other mesenchymal elements) of the heart[47]. It is noteworthy that we found little evidence of interstitial fibrosis in our cardiac-specific VDR knockout while fibrosis is an important feature in the whole animal knockout[48], implying that VDR exerts effects in the fibroblast population that are largely independent of the observed direct effects in the myocyte population.

A variety of studies support a central role for calcineurin signaling in the development of pathological cardiac hypertrophy[34–41]. Calcineurin dephosphorylates and promotes the translocation of NFAT to the nucleus. This sequence of events has been shown to be both necessary and sufficient for the induction of cardiac hypertrophy. MCIP 1 gene expression is tightly controlled by an alternative promoter containing multiple NFAT binding sites in the region upstream of exon 4[29]. Several *in vivo* studies have demonstrated that MCIP 1 expression levels correlate closely with activation of calcineurin/NFAT signaling in the heart. Indeed, MCIP 1 knockout mice display a significant reduction of cardiac hypertrophy induced by pressure overload, neuroendocrine stimulation or exercise[34, 35], suggesting that MCIP 1 mediates calcineurin/NFAT-induced cardiac hypertrophy. We found increased MCIP 1 gene expression in hearts of cardiomyocyte –specific VDR gene-deleted mice and global VDR knockout mice, both of which displayed cardiac hypertrophy. Treatment of rat cardiomyocytes with 1,25 $(OH)_2$ D following induction with ISO led to reduction of MCIP 1 mRNA, protein and promoter activity. Collectively, these results suggest that VDR-dependent anti-hypertrophic activity in the myocyte is linked to suppression of the calcineurin/NFAT/MCIP 1 pathway(s).

These findings add a new and important piece of evidence to incorporate into a growing body of epidemiological[4–13] clinical[14, 17], *in vitro*[18], and whole animal in vivo studies[16] that support the need for adequate vitamin D repletion in the general population to promote cardiovascular health. This takes on particular importance given the high degree of vitamin D insufficiency that exists worldwide[1]. These findings also suggest that targeted use of 1,25 $(OH)_2$ D or its active analogues in clinical situations characterized by aberrant or undesirable hypertrophy of the myocardium may be useful in preventing or slowing the progression of cardiovascular diseases where this is a dominant feature.

Supplementary Material

Refer to Web version on PubMed Central for supplementary material.

Acknowledgments

We acknowledge T.A. McKinsey (University of Colorado Denver), who kindly provided us with the rat MCIP 1 antibody. We are grateful to W. Chang (Veterans Affairs Medical Center, UCSF) for assistance with the PTH assay. We acknowledge the assistance of Y. Zhang (Institute Pasteur of Shanghai, Chinese Academy of Sciences) in the preparation of mice used in these studies, R. Shaw (Dept. of Cardiology, UCSF) for advice on cardiomyocyte

NIH-PA Author Manuscript

NIH-PA Author Manuscript

NIH-PA Author Manuscript

preparation, and C. Barker and A. Williams (UCSF Gladstone Genomics Core) for help with the gene array analysis.

Sources of Funding

This study was supported by HL45637 from the NIH, grants from the Center for D-receptor Activation Research (CeDAR) Program and the ExtenD Program of Abbott Laboratories (D.G.G.), and HL096047 (S.C.).

References

1. Holick MF. Vitamin D deficiency. N Engl J Med. 2007; 357(3):266–281. [PubMed: 17634462]
2. Haussler MR, Haussler CA, Bartik L, Whitfield GK, Hsieh JC, Slater S, Jurutka PW. Vitamin D receptor: molecular signaling and actions of nutritional ligands in disease prevention. Nutr Rev. 2008; 66 Suppl 2(10):S98–S112. [PubMed: 18844852]
3. Rostand SG. Ultraviolet light may contribute to geographic and racial blood pressure differences. Hypertension. 1997; 30(2 Pt 1):150–156. [PubMed: 9260973]
4. Forman JP, Curhan GC, Taylor EN. Plasma 25-hydroxyvitamin D levels and risk of incident hypertension among young women. Hypertension. 2008; 52:828–832. [PubMed: 18838623]
5. Forman JP, Giovannucci E, Holmes MD, Bischoff-Ferrari HA, Tworoger SS, Willett WC, Curhan GC. Plasma 25-hydroxyvitamin D levels and risk of incident hypertension. Hypertension. 2007; 49:1063–1069. [PubMed: 17372031]
6. Pilz S, Tomaschitz A, Ritz E, Pieber TR. Vitamin D status and arterial hypertension: a systematic review. Nature reviews. 2009
7. Chiu KC, Chu A, Go VL, Saad MF. Hypovitaminosis D is associated with insulin resistance and beta cell dysfunction. Am J Clin Nutr. 2004; 79:820–825. [PubMed: 15113720]
8. Ford ES, Ajani UA, McGuire LC, Liu S. Concentrations of serum vitamin D and the metabolic syndrome among U.S. adults. Diabetes Care. 2005; 28:1228–1230. [PubMed: 15855599]
9. Isaia G, Giorgino R, Adami S. High prevalence of hypovitaminosis D in female type 2 diabetic population. Diabetes Care. 2001; 24:1496. [PubMed: 11473093]
10. Pittas AG, Lau J, Hu FB, Dawson-Hughes B. The role of vitamin D and calcium in type 2 diabetes. A systematic review and meta-analysis. J Clin Endocrinol Metab. 2007; 92:2017–2029. [PubMed: 17389701]
11. Fahrleitner A, Dobnig H, Obernosterer A, Pilger E, Leb G, Weber K, Kudlacek S, Obermayer-Pietsch BM. Vitamin D deficiency and secondary hyperparathyroidism are common complications in patients with peripheral arterial disease. J Gen Intern Med. 2002; 17:663–669. [PubMed: 12220361]
12. Pilz S, Marz W, Wellnitz B, Seelhorst U, Fahrleitner-Pammer A, Dimai HP, Boehm BO, Dobnig H. Association of vitamin D deficiency with heart failure and sudden cardiac death in a large cross-sectional study of patients referred for coronary angiography. J Clin Endocrinol Metab. 2008; 93:3927–3935. [PubMed: 18682515]
13. Zittermann A, Schleithoff SS, Tenderich G, Berthold HK, Korfer R, Stehle P. Low vitamin D status: a contributing factor in the pathogenesis of congestive heart failure? J Am Coll Cardiol. 2003; 41:105–112. [PubMed: 12570952]
14. Pfeifer M, Begerow B, Minne HW, Nachtigall D, Hansen C. Effects of a short-term vitamin D(3) and calcium supplementation on blood pressure and parathyroid hormone levels in elderly women. J Clin Endocrinol Metab. 2001; 86:1633–1637. [PubMed: 11297596]
15. Lind L, Wengle B, Ljunghall S. Blood pressure is lowered by vitamin D (alphacalcidol) during long-term treatment of patients with intermittent hypercalcaemia. A double-blind, placebo-controlled study. Acta Med Scand. 1987; 222:423–427. [PubMed: 3321926]
16. Bodyak N, Ayus JC, Achinger S, Shivalingappa V, Ke Q, Chen YS, Rigor DL, Stillman I, Tamez H, Kroeger PE, Wu-Wong RR, Karumanchi SA, Thadhani R, Kang PM. Activated vitamin D attenuates left ventricular abnormalities induced by dietary sodium in Dahl salt-sensitive animals. Proc Natl Acad Sci U S A. 2007; 104:16810–16815. [PubMed: 17942703]

NIH-PA Author Manuscript

NIH-PA Author Manuscript

NIH-PA Author Manuscript

17. Park CW, Oh YS, Shin YS, Kim CM, Kim YS, Kim SY, Choi EJ, Chang YS, Bang BK. Intravenous calcitriol regresses myocardial hypertrophy in hemodialysis patients with secondary hyperparathyroidism. Am J Kidney Dis. 1999; 33:73–81. [PubMed: 9915270]

18. Wu J, Garami M, Cheng T, Gardner DG. 1,25(OH)2 vitamin D3, and retinoic acid antagonize endothelin-stimulated hypertrophy of neonatal rat cardiac myocytes. J Clin Invest. 1996; 97:1577–1588. [PubMed: 8601621]

19. Li YC, Kong J, Wei M, Chen ZF, Liu SQ, Cao LP. 1,25-Dihydroxyvitamin D(3) is a negative endocrine regulator of the renin-angiotensin system. J Clin Invest. 2002; 110:229–238. [PubMed: 12122115]

20. Xiang W, Kong J, Chen S, Cao LP, Qiao G, Zheng W, Liu W, Li X, Gardner DG, Li YC. Cardiac hypertrophy in vitamin D receptor knockout mice: role of the systemic and cardiac renin-angiotensin systems. Am J Physiol Endocrinol Metab. 2005; 288:E125–E132. [PubMed: 15367398]

21. Li YC, Pirro AE, Amling M, Delling G, Baron R, Bronson R, Demay MB. Targeted ablation of the vitamin D receptor: an animal model of vitamin D-dependent rickets type II with alopecia. Proc Natl Acad Sci U S A. 1997; 94:9831–9835. [PubMed: 9275211]

22. Andersson P, Rydberg E, Willenheimer R. Primary hyperparathyroidism and heart disease--a review. Eur Heart J. 2004; 25:1776–1787. [PubMed: 15474692]

23. Rodriguez CI, Buchholz F, Galloway J, Sequerra R, Kasper J, Ayala R, Stewart AF, Dymecki SM. High-efficiency deleter mice show that FLPe is an alternative to Cre-loxP. Nat Genet. 2000; 25:139–140. [PubMed: 10835623]

24. Chen J, Kubalak SW, Chien KR. Ventricular muscle-restricted targeting of the RXRalpha gene reveals a non-cell-autonomous requirement in cardiac chamber morphogenesis. Development (Cambridge, England). 1998; 125:1943–1949.

25. Vincent SD, Robertson EJ. Highly efficient transgene-independent recombination directed by a maternally derived SOX2CRE transgene. Genesis. 2003; 37:54–56. [PubMed: 14595840]

26. O'Connell TD, Rodrigo MC, Simpson PC. Isolation and culture of adult mouse cardiac myocytes. Methods Mol Biol. 2007; 357:271–296. [PubMed: 17172694]

27. Zhang Y, Takagawa J, Sievers RE, Khan MF, Viswanathan MN, Springer ML, Foster E, Yeghiazarians Y. Validation of the wall motion score and myocardial performance indexes as novel techniques to assess cardiac function in mice after myocardial infarction. Am J Physiol Heart Circ Physiol. 2007; 292:H1187–H1192. [PubMed: 17028161]

28. Xu J, Kimball TR, Lorenz JN, Brown DA, Bauskin AR, Klevitsky R, Hewett TE, Breit SN, Molkentin JD. GDF15/MIC-1 functions as a protective and antihypertrophic factor released from the myocardium in association with SMAD protein activation. Circ Res. 2006; 98:342–350. [PubMed: 16397142]

29. Yang J, Rothermel B, Vega RB, Frey N, McKinsey TA, Olson EN, Bassel-Duby R, Williams RS. Independent signals control expression of the calcineurin inhibitory proteins MCIP1 and MCIP2 in striated muscles. Circ Res. 2000; 87:E61–E68. [PubMed: 11110780]

30. Friddle CJ, Koga T, Rubin EM, Bristow J. Expression profiling reveals distinct sets of genes altered during induction and regression of cardiac hypertrophy. Proc Natl Acad Sci U S A. 2000; 97:6745–6750. [PubMed: 10829065]

31. Chien KR, Zhu H, Knowlton KU, Miller-Hance W, van-Bilsen M, O'Brien TX, Evans SM. Transcriptional regulation during cardiac growth and development. Annu Rev Physiol. 1993; 55:77–95. [PubMed: 8466192]

32. Knowles JW, Esposito G, Mao L, Hagaman JR, Fox JE, Smithies O, Rockman HA, Maeda N. Pressure-independent enhancement of cardiac hypertrophy in natriuretic peptide receptor A-deficient mice. J Clin Invest. 2001; 107:975–984. [PubMed: 11306601]

33. Holtwick R, van Eickels M, Skryabin BV, Baba HA, Bubikat A, Begrow F, Schneider MD, Garbers DL, Kuhn M. Pressure-independent cardiac hypertrophy in mice with cardiomyocyte-restricted inactivation of the atrial natriuretic peptide receptor guanylyl cyclase-A. J Clin Invest. 2003; 111:1399–1407. [PubMed: 12727932]

34. Sanna B, Brandt EB, Kaiser RA, Pfluger P, Witt SA, Kimball TR, van Rooij E, De Windt LJ, Rothenberg ME, Tschop MH, Benoit SC, Molkentin JD. Modulatory calcineurin-interacting

NIH-PA Author Manuscript

NIH-PA Author Manuscript

NIH-PA Author Manuscript

proteins 1 and 2 function as calcineurin facilitators in vivo. Proc Natl Acad Sci U S A. 2006; 103:7327–7332. [PubMed: 16648267]

35. Vega RB, Rothermel BA, Weinheimer CJ, Kovacs A, Naseem RH, Bassel-Duby R, Williams RS, Olson EN. Dual roles of modulatory calcineurin-interacting protein 1 in cardiac hypertrophy. Proc Natl Acad Sci U S A. 2003; 100:669–674. [PubMed: 12515860]
36. Bourajjaj M, Armand AS, da Costa Martins PA, Weijts B, van der Nagel R, Heeneman S, Wehrens XH, De Windt LJ. NFATc2 is a necessary mediator of calcineurin-dependent cardiac hypertrophy and heart failure. J Biol Chem. 2008; 283:22295–22303. [PubMed: 18477567]
37. Bueno OF, Wilkins BJ, Tymitz KM, Glascock BJ, Kimball TF, Lorenz JN, Molkentin JD. Impaired cardiac hypertrophic response in Calcineurin Abeta -deficient mice. Proc Natl Acad Sci U S A. 2002; 99:4586–4591. [PubMed: 11904392]
38. De Windt LJ, Lim HW, Bueno OF, Liang Q, Delling U, Braz JC, Glascock BJ, Kimball TF, del Monte F, Hajjar RJ, Molkentin JD. Targeted inhibition of calcineurin attenuates cardiac hypertrophy in vivo. Proc Natl Acad Sci U S A. 2001; 98:3322–3327. [PubMed: 11248077]
39. Wilkins BJ, De Windt LJ, Bueno OF, Braz JC, Glascock BJ, Kimball TF, Molkentin JD. Targeted disruption of NFATc3, but not NFATc4, reveals an intrinsic defect in calcineurin-mediated cardiac hypertrophic growth. Mol Cell Biol. 2002; 22:7603–7613. [PubMed: 12370307]
40. Zou Y, Hiroi Y, Uozumi H, Takimoto E, Toko H, Zhu W, Kudoh S, Mizukami M, Shimoyama M, Shibasaki F, Nagai R, Yazaki Y, Komuro I. Calcineurin plays a critical role in the development of pressure overload-induced cardiac hypertrophy. Circulation. 2001; 104:97–101. [PubMed: 11435345]
41. Wilkins BJ, Dai YS, Bueno OF, Parsons SA, Xu J, Plank DM, Jones F, Kimball TR, Molkentin JD. Calcineurin/NFAT coupling participates in pathological, but not physiological, cardiac hypertrophy. Circ Res. 2004; 94:110–118. [PubMed: 14656927]
42. Zittermann A, Schleithoff SS, Koerfer R. Putting cardiovascular disease and vitamin D insufficiency into perspective. Br J Nutr. 2005; 94:483–492. [PubMed: 16197570]
43. Heyliger A, Tangpricha V, Weber C, Sharma J. Parathyroidectomy decreases systolic and diastolic blood pressure in hypertensive patients with primary hyperparathyroidism. Surgery. 2009; 146:1042–1047. [PubMed: 19958931]
44. Piovesan A, Molineri N, Casasso F, Emmolo I, Ugliengo G, Cesario F, Borretta G. Left ventricular hypertrophy in primary hyperparathyroidism. Effects of successful parathyroidectomy. Clinical endocrinology. 1999; 50:321–328. [PubMed: 10435057]
45. Chen S, Law CS, Gardner DG. Vitamin D-dependent suppression of endothelin-induced vascular smooth muscle cell proliferation through inhibition of CDK2 activity. J Steroid Biochem Mol Biol. 2009
46. Oh J, Weng S, Felton SK, Bhandare S, Riek A, Butler B, Proctor BM, Petty M, Chen Z, Schechtman KB, Bernal-Mizrachi L, Bernal-Mizrachi C. 1,25(OH)2 vitamin d inhibits foam cell formation and suppresses macrophage cholesterol uptake in patients with type 2 diabetes mellitus. Circulation. 2009; 120:687–698. [PubMed: 19667238]
47. Chen S, Glenn DJ, Ni W, Grigsby CL, Olsen K, Nishimoto M, Law CS, Gardner DG. Expression of the vitamin d receptor is increased in the hypertrophic heart. Hypertension. 2008; 52:1106–1112. [PubMed: 18936343]
48. Rahman A, Hershey S, Ahmed S, Nibbelink K, Simpson RU. Heart extracellular matrix gene expression profile in the vitamin D receptor knockout mice. J Steroid Biochem Mol Biol. 2007; 103:416–419. [PubMed: 17275288]

NIH-PA Author Manuscript

NIH-PA Author Manuscript

NIH-PA Author Manuscript

Clinically, vitamin D has usually been linked to disorders of the skeletal system where vitamin D deficiency is associated an increase in fracture risk. More recently, it has become clear that vitamin D has important actions in non-classic target tissues like the immune system, heart and vasculature. This study provides the first demonstration for a direct effect of the liganded vitamin D receptor (VDR) in the heart. Using a specially engineered mouse model, we have produced selective deletion of the VDR in the cardiac myocyte. This deletion leads to an increase in heart weight-to-body weight ratio, an increase in myocyte size without interstitial fibrosis and activation of a gene expression program that is typically associated with hypertrophy and fibrosis. Of note, deletion of the VDR leads to activation of a signaling molecule called the modulatory calcineurin inhibitory protein 1 (MCIP 1) that is known play a role in the pro-hypertrophic, calcineurin-dependent signaling cascade. Treatment of myocytes in culture with a potent vitamin D metabolite leads to a reduction in MCIP 1 gene expression. These findings present the first definitive support for a direct beneficial effect of vitamin D and its metabolites in the heart. They imply that vitamin D sufficiency, acquired through diet or ultraviolet light, is important for cardiovascular health and suggest that more potent vitamin D analogues may be of value in the treatment of cardiac disorders associated with myocyte hypertrophy.

NIH-PA Author Manuscript

NIH-PA Author Manuscript

NIH-PA Author Manuscript

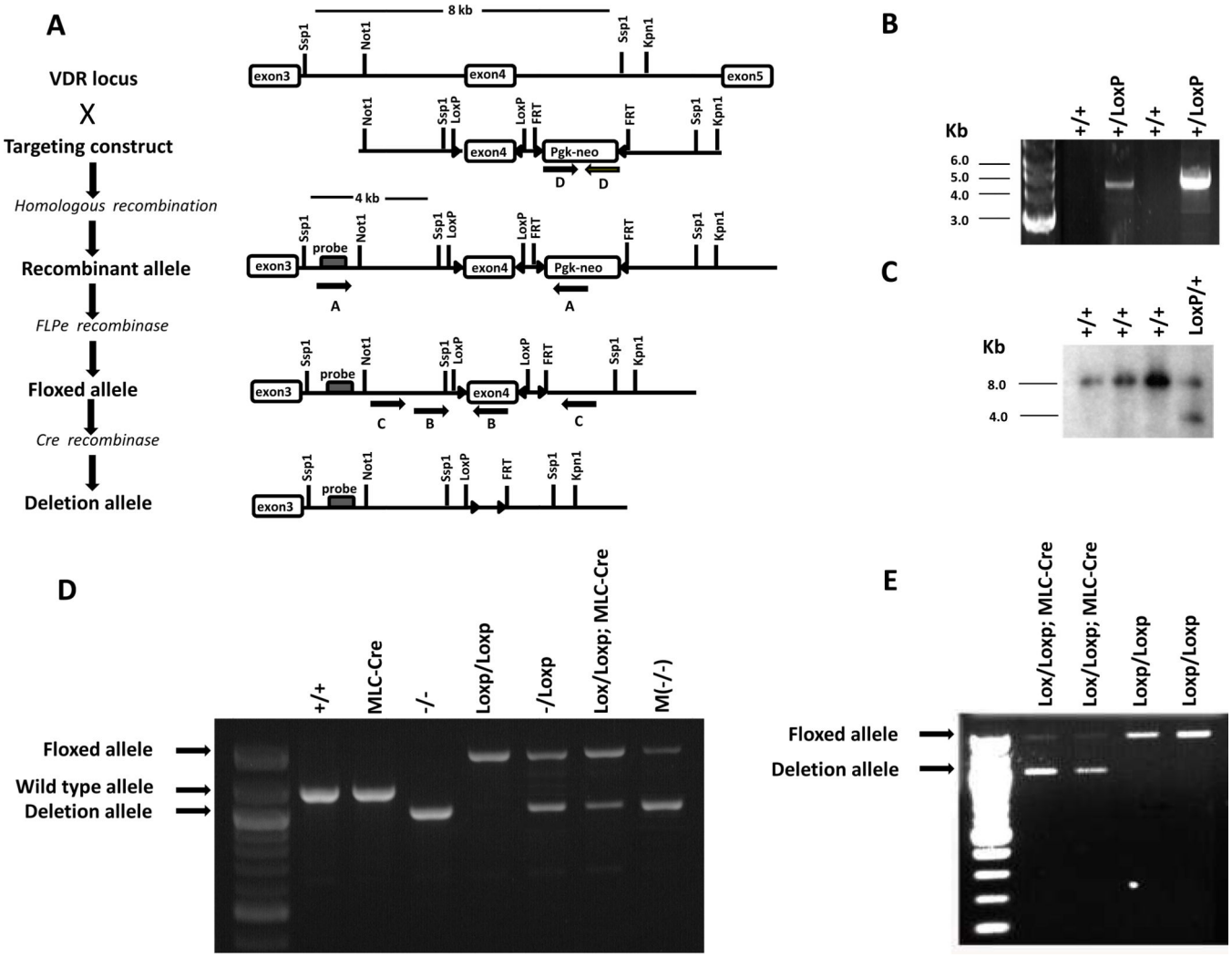

Fig. 1.

Generation of cardiomyocyte-specific VDR knockout mice. **A**: Schematic diagram of targeting strategy. Two loxp sites flanking VDR exon 4 and two FRT sites flanking the phosphoglycerol kinase-neomycin (Pgk-neo) resistance gene in the targeting vector were incorporated into the recombinant allele. Flpe recombinase removed the neo cassette by cutting at the FRT sites. Cre recombinase-mediated elimination of exon 4 deleted the second zinc finger region of VDR DNA binding domain, leading to a knockout allele. **B**: Two positive embryonic stem (ES) cell clones containing the recombinant allele identified by PCR using primer pair A (arrows show the primer sites in panel **A**). **C**: Genomic DNA from ES cells was restricted with Ssp1 and subjected to Southern blot analysis (probe location shown in panel **A**). **D**: Wild type, recombinant and deletion alleles in F8 generation mice were identified by PCR using left ventricular genomic DNA as template and primer pair C, $VDR^{-/-}$ (−/−) and MLC-Cre/$VDR^{loxP/-}$ [M(−/−)]. **E**: Recombinant and deletion alleles were characterized by PCR using genomic DNA from isolated left ventricular myocytes and primer pair C.

NIH-PA Author Manuscript

NIH-PA Author Manuscript

NIH-PA Author Manuscript

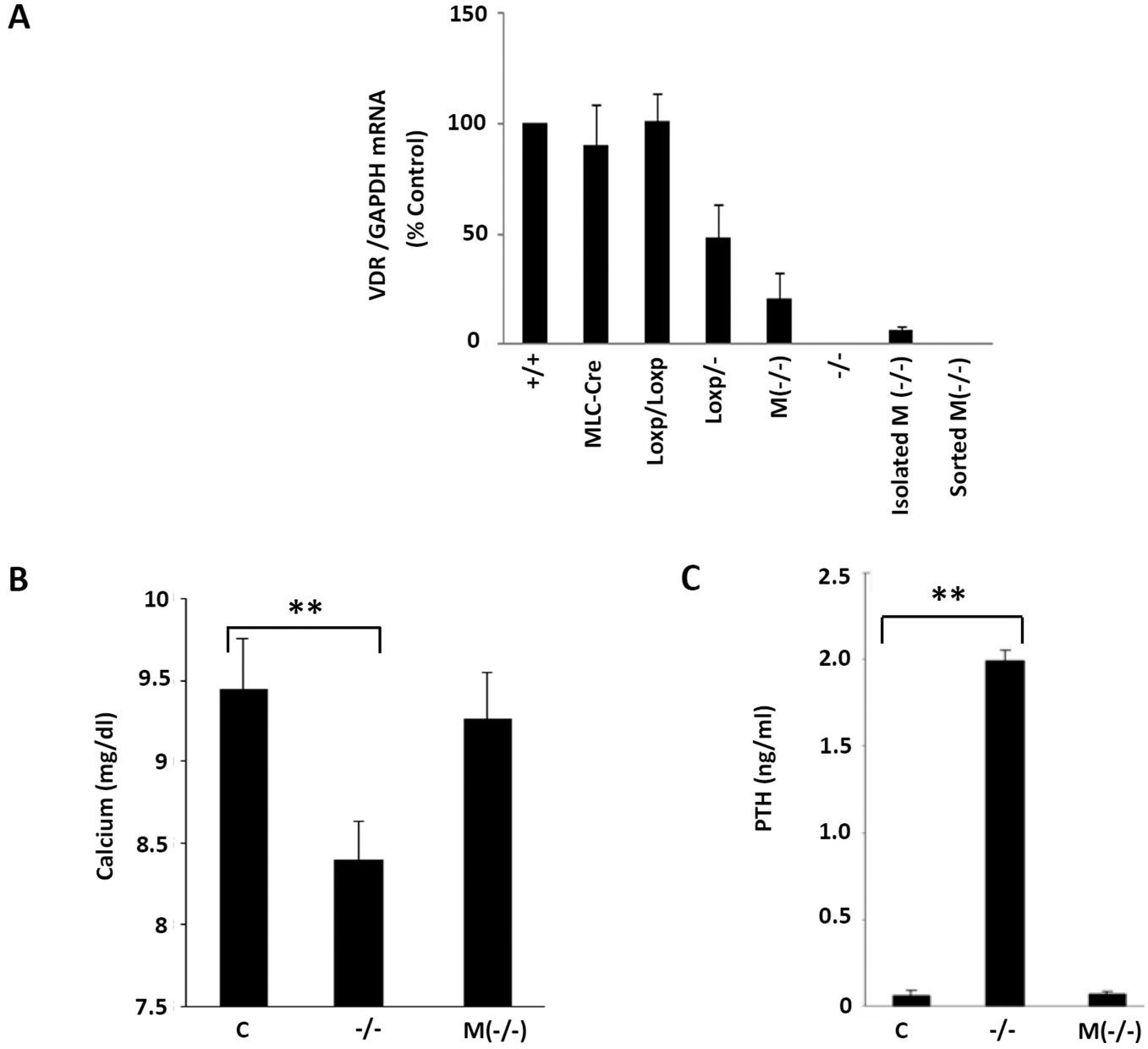

Fig. 2.

Demonstration of normal plasma calcium and PTH levels in mice with deletion of VDR in cardiomyocytes. **A**: RT-PCR analyses of VDR and GAPDH mRNA levels in isolated and sorted left ventricular myocytes from mice with different genotypes, as indicated. **B**: Determination of the plasma calcium levels from $VDR^{loxP/-}$ (C), (−/−) and M(−/−) mice. **C**. Measurement of plasma PTH levels from same mice. Bar graphs display mean and standard deviation from n=8–10 per group. **P<0.01 vs. control.

NIH-PA Author Manuscript
NIH-PA Author Manuscript
NIH-PA Author Manuscript

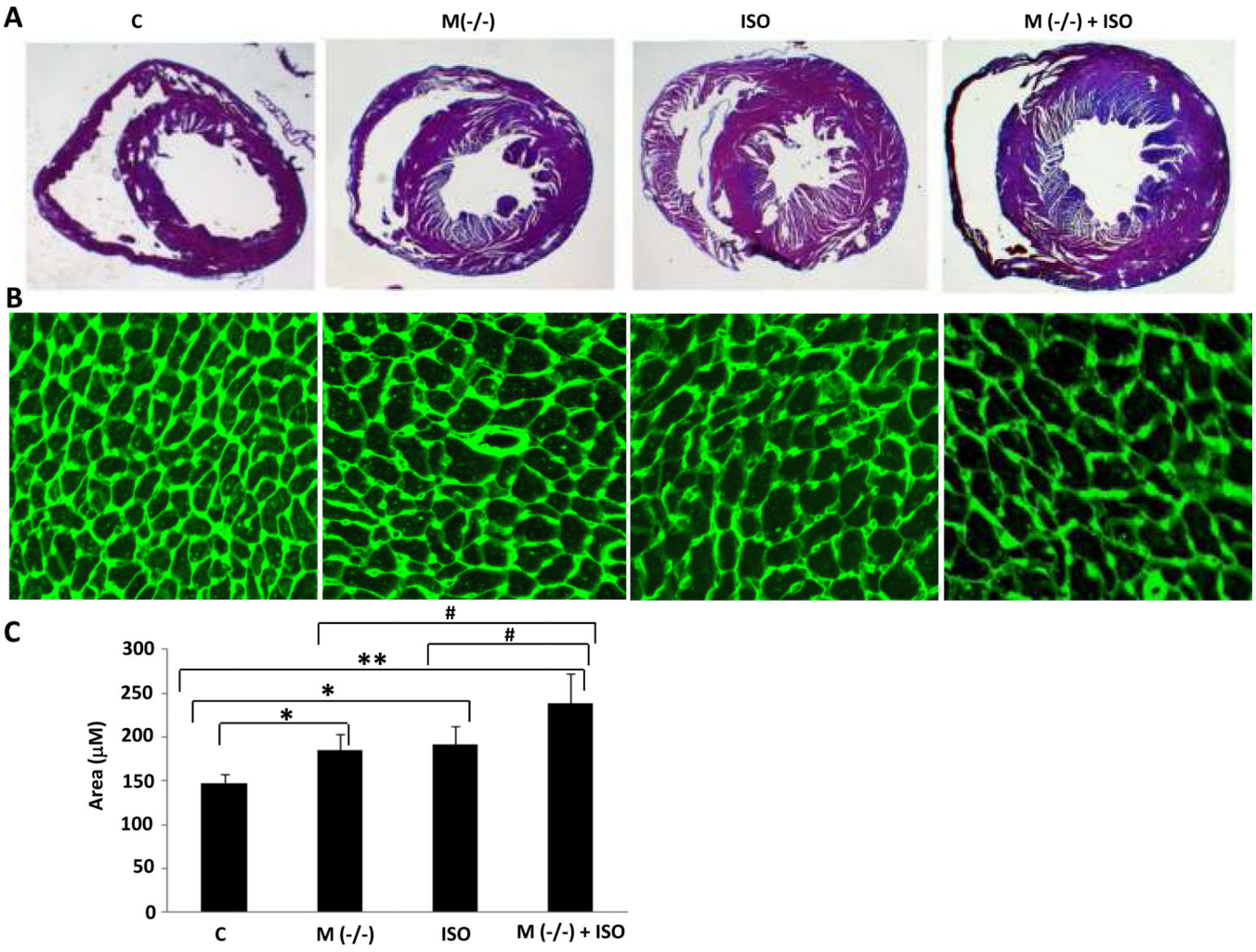

Fig. 3.

Cardiac hypertrophy in cardiomyocyte-specific VDR knockout mice. **A**: Left ventricular sections of hearts from mice with genotype indicated were stained by H&E. Representative sections are shown. **B**: Cardiac sections were stained with FITC-WGA, which delineates cell dimensions by staining glycoprotein enveloping individual myocytes. Representative photomicrographs are shown. **C**: Individual myocyte size was assessed using ImageJ (NIH). The mean myocyte area was evaluated by measurement of 400 cells per heart (4–5 heart per genotype). Bar graphs displaying mean and standard deviation from 8–12 mice per group are shown. *P<0.05, **P<0.01 vs. control. $^{\#}$P<0.05 vs. M(−/−) + ISO.

NIH-PA Author Manuscript

NIH-PA Author Manuscript

NIH-PA Author Manuscript

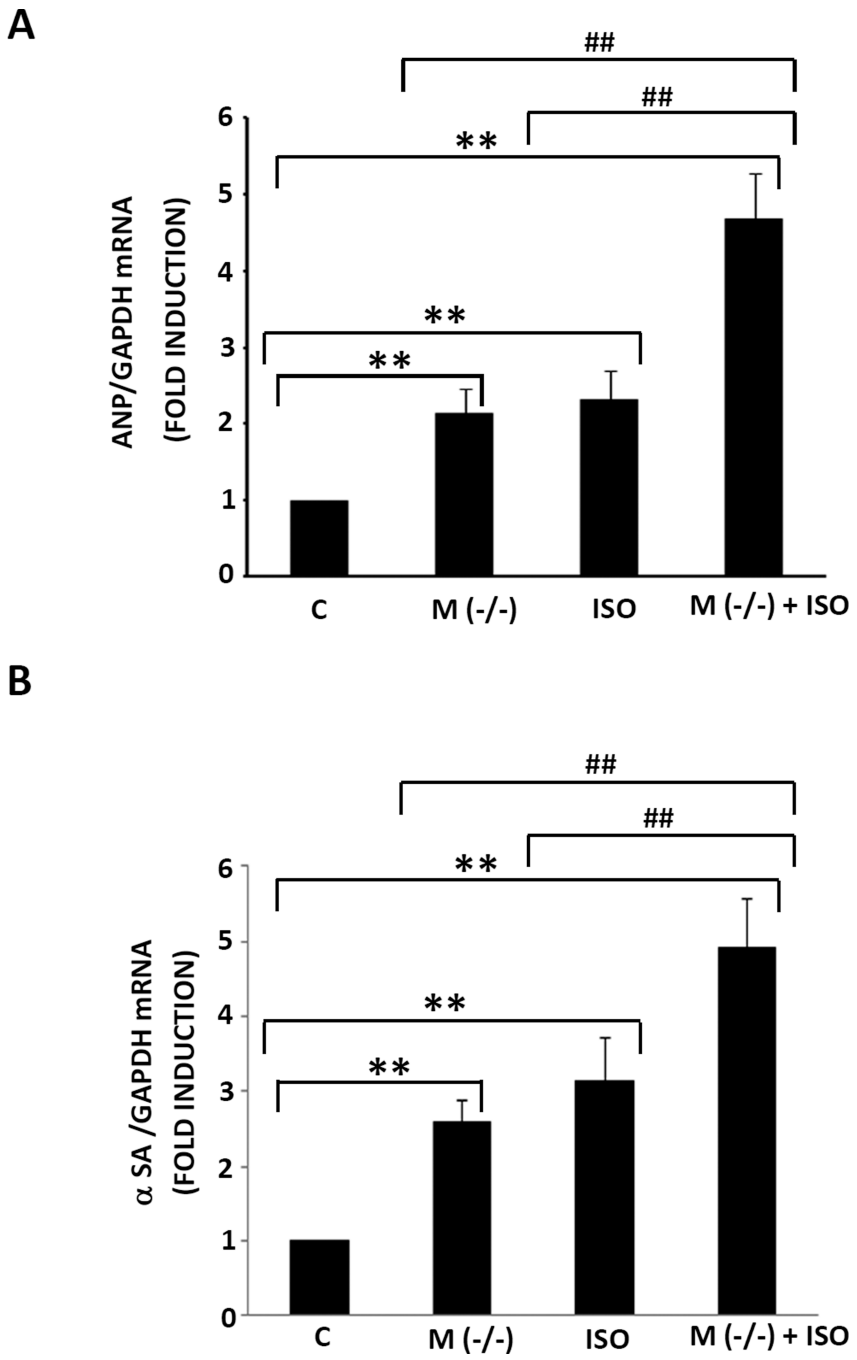

Fig. 4.

Increased expression of hypertrophic gene markers in cardiomyocyte-specific VDR knockout mice. **A**: Total RNA was extracted from left ventricular tissue and RT-PCR was carried out to measure ANP and GAPDH mRNA levels. ANP expression was normalized to GAPDH levels. **B**: Quantitative PCR was performed to determine the αSA and GAPDH mRNA levels of each transcript. αSA mRNA level was normalized to GAPDH mRNA expression. Bar graphs demonstrate mean and standard deviation from 6–8 samples per group. **P<0.01 vs. control. $^{\#\#}$P<0.01 vs. M(−/−) + ISO.

NIH-PA Author Manuscript

NIH-PA Author Manuscript

NIH-PA Author Manuscript

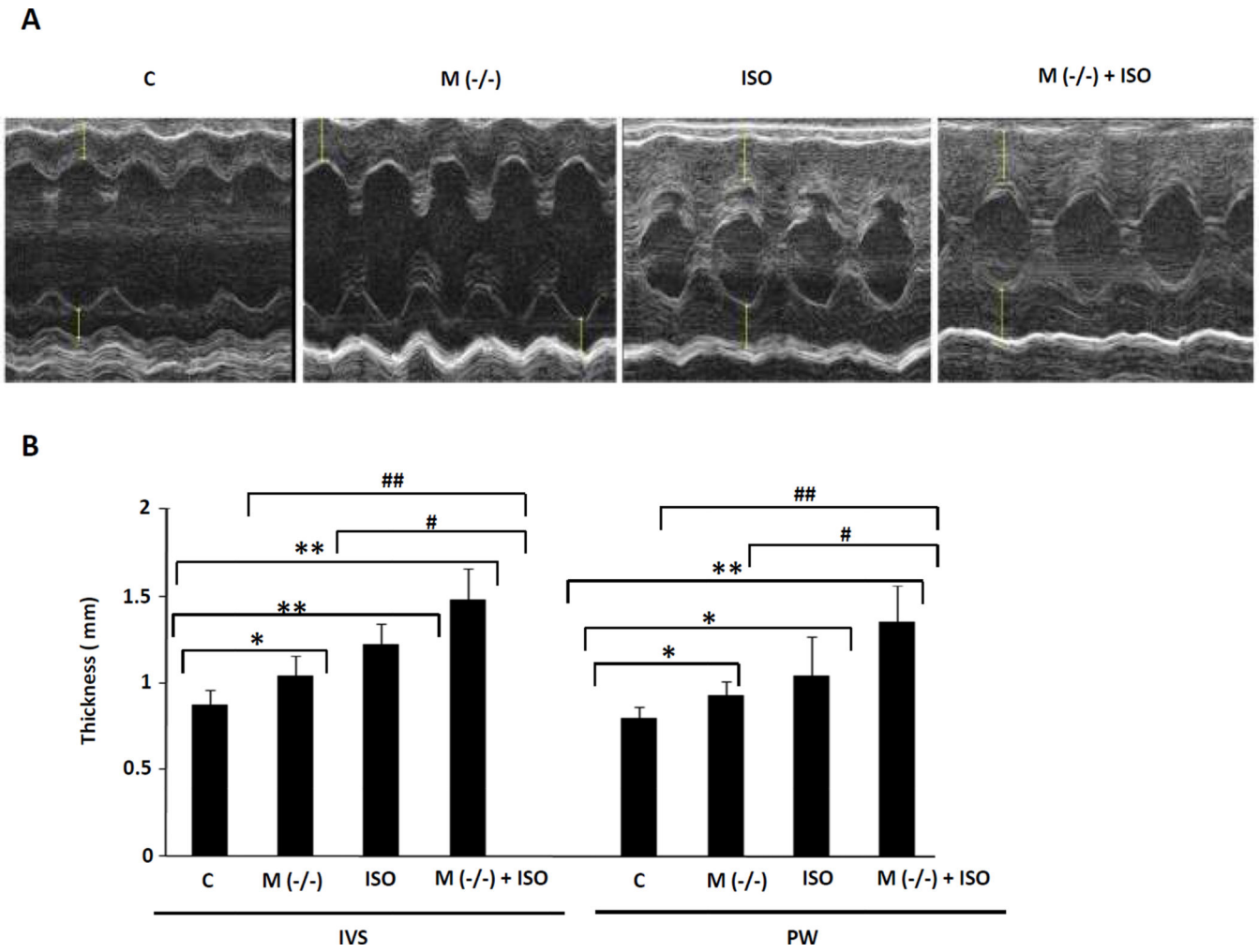

Fig. 5.

Echocardiography of mice with cardiomyocyte-specific VDR knockout in presence or absence of ISO infusion. **A**: Representative M-mode images are demonstrated. **B**: Thickness of interventricular septum (IVS) and posterior wall (PW) was measured and bar graphs displaying mean and standard deviation from n=6–8 per group are shown. *P<0.05, **P<0.01 vs. control. $^{\#}$P<0.05, $^{\#\#}$P<0.01 vs. M(−/−) + ISO.

NIH-PA Author Manuscript

NIH-PA Author Manuscript

NIH-PA Author Manuscript

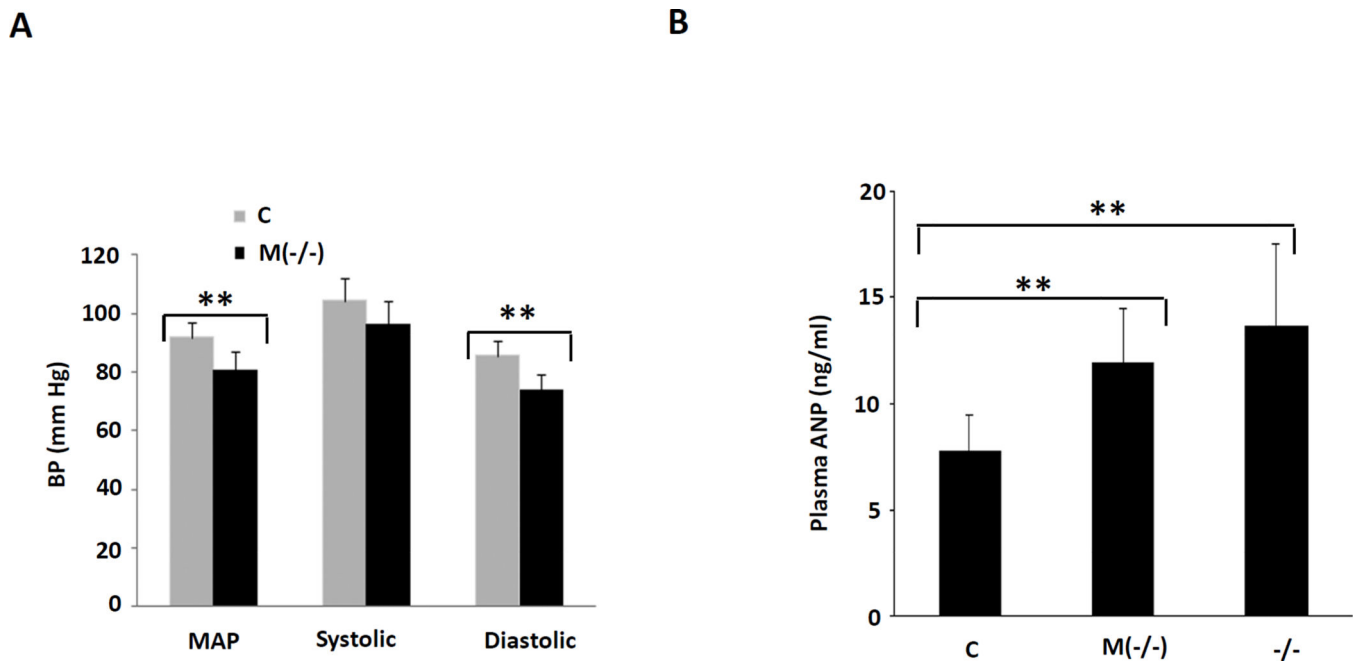

Fig. 6.

Reduction of blood pressure and increase in plasma ANP level in cardiomyocyte-specific VDR gene knockout mice. **A**: Mouse blood pressure was measured using tail-cuff technique described in Methods. The histogram shows the pooled data from 6–8 animals in each group. **B**: Plasma ANP level (n=10–12 each group) was determined by ANP RIA kit. C, control; M(−/−), cardiac specific VDR knockout; −/−, whole animal knockout. **P<0.01 vs. control.

NIH-PA Author Manuscript
NIH-PA Author Manuscript
NIH-PA Author Manuscript

A

Gene names	Gene descriptions	Fold Change	P value
Nppb	Natriuretic peptide precursor type B	2.88	0.0003
Nppa	Natriuretic peptide precursor type A	2.46	0.0344
MCIP1 (Rcan1)	Regulator of calcineurin 1	2.1	0.001
Dpt	Dermatopontin	2.07	0.001
Mgp	Matrix Gla protein	1.96	0.019
Acta2	Actin, alpha 2, smooth muscle, aorta	1.9	0.037
Lum	Lumican	1.89	0.010
Cyp1b1	Cytochrome P450, family 1b1	1.78	0.008
2810474O19Rik	RIKEN cDNA 1700038P13 gene	1.66	0.045

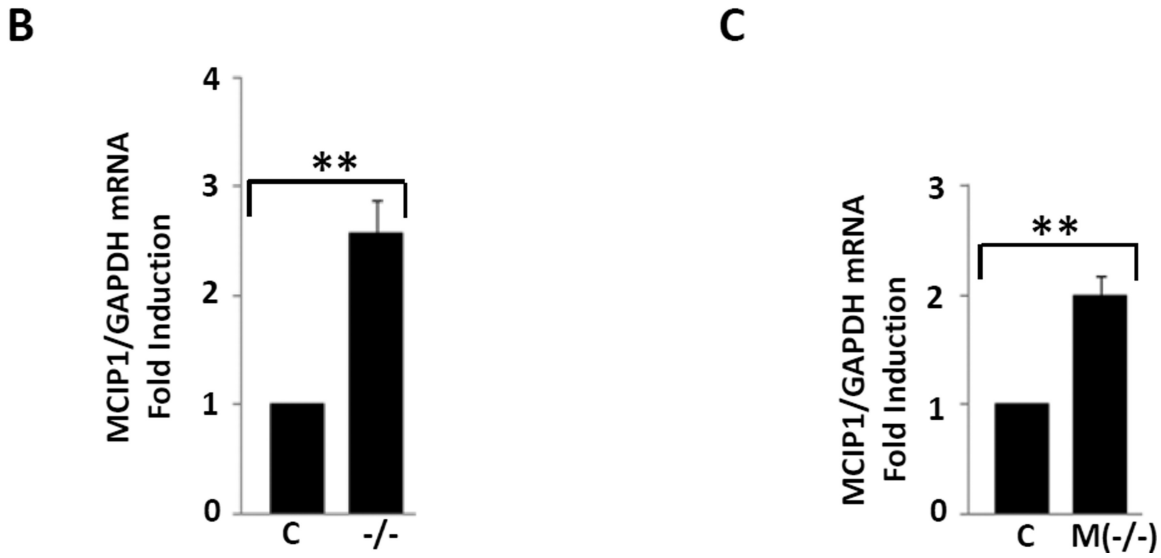

Fig. 7.

MCIP 1 is a potential mediator of cardiac hypertrophy in VDR-deficient myocytes. **A**: Gene array analysis. Total mRNA was obtained from isolated ventricular myocytes of cardiomyocyte-specific VDR knockout vs. control mice. **B&C**: MCIP 1 mRNA levels were significantly increased in heart tissue from $VDR^{-/-}$ mice and myocytes isolated from cardiomyocyte-specific VDR knockout mice. **P<0.01 vs. control (n=5 per group).

NIH-PA Author Manuscript

NIH-PA Author Manuscript

NIH-PA Author Manuscript

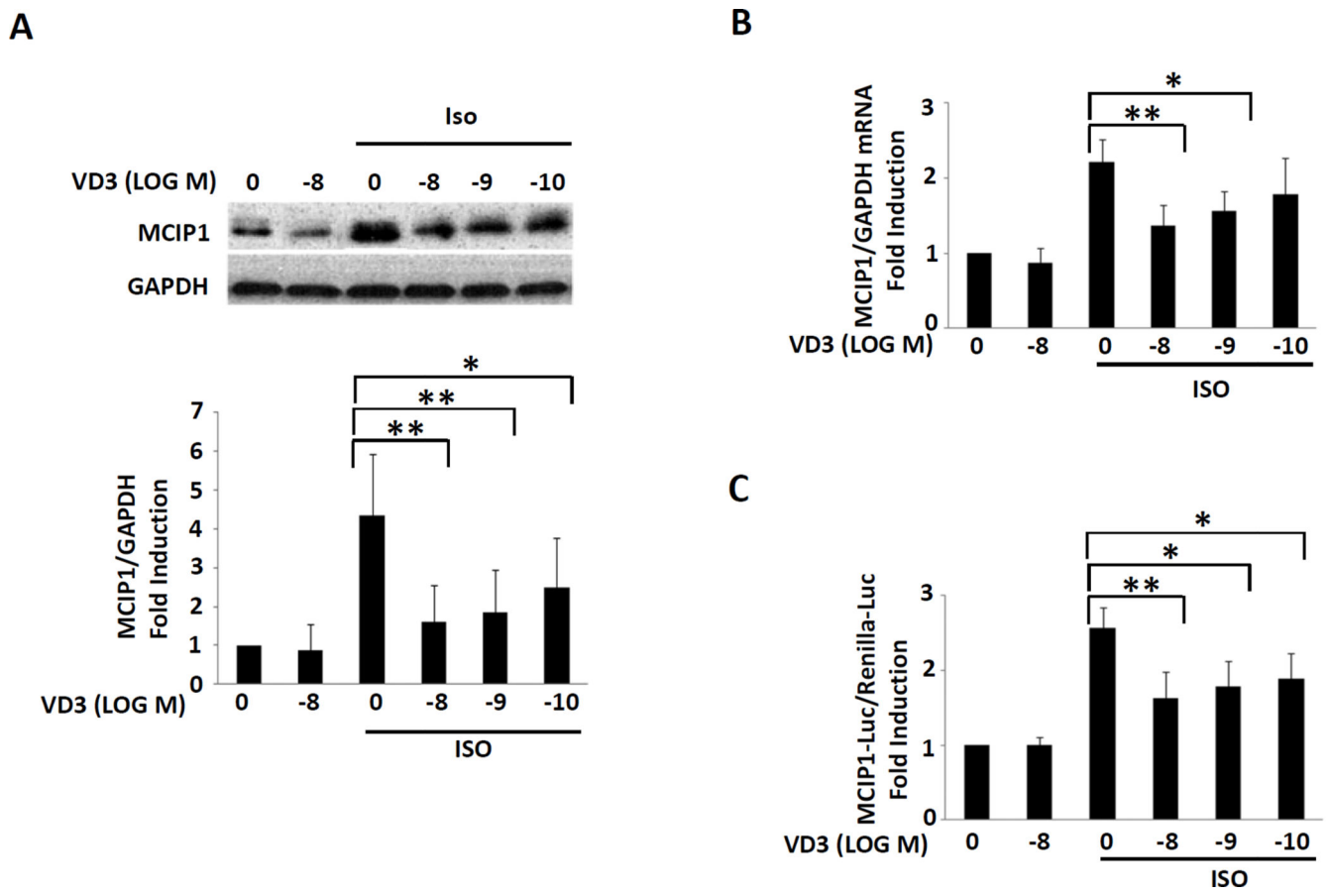

Fig. 8.

1,25 $(OH)_2$ D (VD3) partially inhibited ISO-induced MCIP 1 protein, mRNA and promoter activities in rat neonatal cardiomyocytes. **A**: MCIP 1 protein expression was normalized to GAPDH levels (representative results shown in the upper panel, pooled data shown in the lower panel). **B**: MCIP 1 mRNA levels measured by RT-PCR were normalized to GAPDH levels. **C**: Mouse MCIP 1-Luc activities were normalized to Renilla-Luc activities. *P<0.05, **P<0.01 vs. ISO alone (n=3–5 per group).

NIH-PA Author Manuscript

NIH-PA Author Manuscript

NIH-PA Author Manuscript

Table 1

Cardiomyocyte-specific knockout of the VDR gene results in left ventricular hypertrophy. Body weight (BW), left ventricular weight (LVW), LVW/BW and heart rate (HR) measurements (n=8–12 per group).

Animal	BW (g)	LVW (mg)	LVW/BW (mg/g)	HR (bpm)
C	39.1 ± 7.0	105.7 ± 8.1	2.69 ± 0.21	679.7 ± 147.0
M(−/ −)	38.5 ± 3.5	121.8 ± 12.3** #	3.16 ± 0.27** #	676.7 ± 91.7
ISO	40.4 ± 4.2	132.1 ± 11.8** #	3.27 ± 0.20** #	686.3 ± 42.0
M(−/−) + ISO	40.3 ± 2.8	150.3 ± 9.1**	3.78 ± 0.37**	737.0 ± 56.0

** P<0.01 vs. Control;

# P<0.05 vs. M(−/−) + ISO group